Table IV. Summary of Crystallographic Information

	6b	7a	7b
formula	$C_{11}H_{13}NO$	$C_{12}H_{11}NO$	$C_{14}H_{15}NO$
formula weight	175.23	185.23	213.28
crystal size (mm)	0.10, 0.25, 0.38	0.05, 0.20, 0.35	0.12, 0.30, 0.36
a (Å)	7.690 (5)	6.136 (6)	7.588 (5)
b (Å)	10.754 (3)	20.448 (7)	13.466 (7)
c (Å)	11.442 (4)	7.610 (2)	19.694 (10)
α (deg)			69.19 (4)
β (deg)			79.14 (5)
γ (deg)			74.39 (5)
V (Å^3)	946	954	1802
Z	4	4	6
space group (no.)	$P2_12_12_1$ (19)	$P2_12_12_1$ (19)	$P\bar{1}$ (2)
μ (cm^{-1})	0.72	0.50	0.69
scan rate (deg min^{-1})	1.0	0.5-1.0	2.0
2θ(max) (deg)	56	56	40
θ scan width (deg)	1.0	0.5	0.6
no. of reflns (total)	1363	2304	3371
no. of reflns (used)	628	1334	1914
R_1	0.068	0.059	0.070
R_2	0.062	0.065	0.068
goodness of fit	1.62	1.46	1.82

Celite pad and the filtrate cooled to allow crystals to form. The mixture was then filtered to afford 6.74 g (84%) of *N*-tosylazetidine.[46] Detosylation of this material was effected as reported,[47] and the amide **6b** was prepared by using the standard Schotten-Bauman reaction.

c. **X-ray Crystallography.** Experimental details on each of the determinations are summarized in Table IV. Single-crystal X-ray diffraction intensities were collected at ambient temperatures on an Enraf-Nonius CAD4 diffractometer with Mo Kα radiation (λ = 0.7107 Å) and Zr filter. The structure solution and refinement were carried out on a SUN Microsystems 3/160 workstation. Complete details, including listings of atomic coordinates, displacement parameters, all interatomic bond lengths and angles, torsional angles, least-squares plane information, and structure factor amplitudes have been deposited as supplementary material.

Acknowledgment. We thank the University of Alberta and Natural Sciences and Engineering Research Council of Canada for financial support of this work. In addition, we are grateful to Professor J. E. Bertie (Department of Chemistry, University of Alberta) for helpful discussions concerning infrared analysis, to Ms. B. A. Kellogg for the preparation of **8b** and *N*,*N*-dicyanomethyltoluamide, and to Dr. H. Slebocka-Tilk for the preparation of **8a** and *N*-toluoyl-3,3,4,4-tetrafluoropyrrolidine. Finally, Professor E. Knaus, Faculty of Pharmacy, University of Alberta, is acknowledged for his generosity in making available the Bruker AM300 FT NMR spectrometer to V.S. for determining the ^{15}N chemical shifts.

Registry No. 3a, 76059-52-4; **3b**, 102586-88-9; **3c**, 128732-45-6; **3d**, 128732-46-7; **4a**, 103-84-4; **4b**, 579-10-2; **4c**, 6332-98-5; **4d**, 573-26-2; **4e**, 128732-47-8; **5**, 14062-78-3; **5**-^{13}C, 135469-61-3; **5**-^{18}O, 113109-79-8; **6a**, 2453-33-0; **6a**-^{13}C, 135469-64-6; **6b**, 51425-91-3; **6c**, 59746-40-6; **6c**-^{13}C, 135469-62-4; **6c**-^{18}O, 135469-63-5; **6d**, 13707-23-8; **6e**, 63833-44-3; **7a**, 70971-70-9; **7a**-^{13}C, 135469-65-7; **7a**-^{18}O, 135469-66-8; **7b**, 135469-59-9; **8b**, 135469-60-2; bis(trifluoroethyl)amine, 407-01-2; *p*-toluoyl chloride, 874-60-2; azetidine, 503-29-7; *N*-tosyl-*O*-tosyl-3-aminopropanol, 51425-88-8; *N*-tosylazetidine, 7730-45-2.

Supplementary Material Available: Experimental details and tables of atomic coordinates, displacement parameters, all interatomic bond lengths and angles, torsional angles, and least-squares plane information for **6b**, **7a**, and **7b** (47 pages); tables of calculated and observed structure factors for **6b**, **7a**, and **7b** (39 pages). Ordering information is given on any current masthead page.

Tracing Indications of Anomalous Diffusion in Adsorbent-Adsorbate Systems by PFG NMR Spectroscopy

Jörg Kärger*,† and Herbert Spindler‡

Contribution from the Sektion Physik, Universität Leipzig, O-7010 Leipzig, Germany, and Leuna-Werke AG, Abteilung Katalysatoren, O-4220 Leuna, Germany.
Received January 29, 1991

Abstract: PFG (pulsed field gradient) NMR spectroscopy is applied to measure the molecular mean square displacement in various adsorbent-adsorbate systems in dependence on the observation time. Irrespective of the fact that the pore size distribution yields fractal properties, for the investigated active carbons over the accessible space scale ($\gtrsim$1 μm), mass transfer of the adsorbed molecules is found to obey the laws of ordinary diffusion. When molecular mass transfer in beds of zeolite crystallites is investigated, deviations from ordinary diffusion are found. They are to be attributed, however, to the influence of the crystallite boundary and/or the intercrystalline space. It is most likely that the recently observed indication of anomalous diffusion in polycrystalline grains of zeolite ZSM-5 may be attributed to analogous microdynamic processes.

In the last few years, mass transfer in disordered media has attracted the interest of a large number of researchers.[1-6] As yet, the major part of these investigations has been devoted to purely geometrical models, so that there is a remarkable deficiency in our knowledge of mass-transfer phenomena in real systems reflecting the properties predicted by the theory. PFG (pulsed field gradient) NMR spectroscopy has been repeatedly proposed as a most sensitive tool for detecting deviations from ordinary diffusion during mass transfer in adsorbent-adsorbate systems.[5-7] In comparison to other techniques, the PFG NMR method provides a most direct way to measure molecular mean square displacements without any interference with the intrinsic mass transfer phenomena.[8,9]

In the case of ordinary, three-dimensional diffusion, according to Einstein's relation

† Universität Leipzig.
‡ Leuna-Werke AG.

(1) Havlin, S.; Ben-Avraham, D. *Adv. Phys.* **1987**, *36*, 695.
(2) Guyer, R. A. *Phys. Rev. A* **1985**, *32*, 2324.
(3) O'Shaughnessy, B.; Procaccia, I. *Phys. Rev. A* **1985**, *32*, 3073.
(4) Pfeifer, P. *Chimia* **1985**, *39*, 120.
(5) Pfeifer, P. In *Chemistry and Physics of Solid Surfaces VII*; Vanselow, R., Howe, R. F., Eds.; Springer: Berlin, 1988; p 283.
(6) Spindler, H.; Vojta, G. *Z. Chem.* **1988**, *28*, 421.
(7) Jug, G. *Chem. Phys. Lett.* **1986**, *131*, 94.
(8) Stejskal, E. D.; Tanner, J. E. *J. Chem. Phys.* **1965**, *42*, 288.
(9) Kärger, J.; Pfeifer, H.; Heink, W. *Adv. Magn. Reson.* **1988**, *12*, 1.

0002-7863/91/1513-7571$02.50/0

$$\langle r^2(t)\rangle = 6Dt \quad (1)$$

the mean square displacement $\langle r^2(t)\rangle$ is proportional to the observation time t, with D denoting the self-diffusion coefficient. Theoretical considerations show that, for mass transfer in disordered systems, eq 1 may not be valid any longer. It is to be replaced by the more general relation[1,5,10]

$$\langle r^2(t)\rangle = \alpha t^x \quad (2)$$

In the present study, PFG NMR is applied to different adsorbent–adsorbate systems to trace possible deviations from ordinary self-diffusion and to clarify their origin.

Experimental Section

Molecular self-diffusion has been studied by applying ^{1}H PFG NMR. The measurements have been carried out by using the home-built pulse spectrometer FEGRIS at the Physics Department of the Leipzig University. The resonance frequency was 60 MHz, corresponding to a magnetic field of 1.4 T. Molecular mean square displacements have been determined in the conventional way[8,9,11,12] by analyzing the relative intensity $\Psi(\Delta,\delta g)$ of the NMR signal (the "spin echo") in dependence on the applied, time-dependent inhomogeneity of the external magnetic field (the "pulsed field gradients") using the relation

$$\Psi(\Delta,\delta g) = \exp\{-\gamma^2\delta^2 g^2\langle r^2(\Delta)\rangle/6\} \quad (3)$$

In this equation, the quantities γ, δ, g, and Δ denote, respectively, the gyromagnetic ratio ($=2.675 \times 10^8$ T^{-1} s^{-1} for protons) and the width, intensity, and separation of the field gradient pulses. $\langle r^2(\Delta)\rangle$ is the molecular mean square displacement during the interval between the two field gradient pulses. For simplicity, their duration δ is assumed to be much less than the separation Δ between them. It has been demonstrated in ref 13 that eq 3, which originally has been derived for ordinary diffusion,[8,9] is also valid in the case of anomalous diffusion.

The NMR spectrometer FEGRIS allows the application of field gradients with intensities g up to 20 T/m over an interval of 5 ms, maximum. Inserting these data into eq 3 and realizing that, for an unambiguous measurement of the signal attenuation due to diffusion, the exponent should be of the order of 1,[14] one finds the minimum root mean square displacement as accessible by the given device using ^{1}H PFG NMR to be of the order of 0.1 μm. Due to the smaller gyromagnetic ratios, for other NMR active nuclei, this value is still larger.[9,12] However, in general, this estimate does only provide a hypothetical lower limit. This is due to the fact that the application of gradient widths of 5 ms, necessary for the observation of such small displacements, simultaneously implies separation times Δ above this value. Inserting these data ($\Delta >$ 5 ms and $\langle r^2(\Delta)\rangle < (0.1\ \mu\text{m})^2$) into eq 1, one finds that this requirement can only be fulfilled with self-diffusion coefficients of the order of or smaller than 3×10^{-13} m^2 s^{-1}. However, the low molecular mobility in such systems generally leads to so small transverse nuclear magnetic relaxation times (implying such a drastic decay of the NMR spin-echo intensity with increasing observation times)[15] that the application of such large observation times is not possible, at all. Thus, the real minimum molecular displacements as accessible in our experiments turned out to be of the order of 1 μm.

For observation times in the region of milliseconds, the NMR signal has been produced by the application of the rf pulse sequence of the "primary" echo ($\pi/2 - \tau - \pi - \tau$ – spin echo)[8,9], whose intensity is determined by the transverse nuclear magnetic relaxation time. For larger observation times, the "stimulated" echo ($\pi/2 - \tau_1 - \pi/2 - (\tau_2 - \tau_1) - \pi/2 - \tau_1$ – stimulated echo) has been applied.[9,16] In this case, during the interval between the second and third $\pi/2$ pulses, NMR signal attenuation is due to longitudinal rather than to transverse relaxation. Since the longitudinal relaxation times were found to be in the region of tens to hundreds of milliseconds (in contrast to milliseconds for the transverse relaxation times), in this way, observation times over several hundreds of milliseconds have become possible.

As adsorbents, we have applied an active carbon of the type Hydraffin 71 (Lurgi, Germany). The pore size distribution of the used sample has been determined by mercury porosimetry and by evaluating the N_2 adsorption isotherms.[17,18] It is shown in Figure 1. Further on, we have applied laboratory-synthesized zeolites NaX provided by S. P. Zhdanov and N. N. Feoktistova, Leningrad,[19] and ZSM-5 provided by B. Fahlke, Berlin. By microscopic inspection, the zeolite NaX was found to be of uniform crystalline structure, while the adsorbent particles of the applied zeolite ZSM-5 were spherulitic polycrystals. Details of the synthesis of the ZSM-5 species and microphotographs of the crystals and polycrystals, respectively, may be found in ref 20.

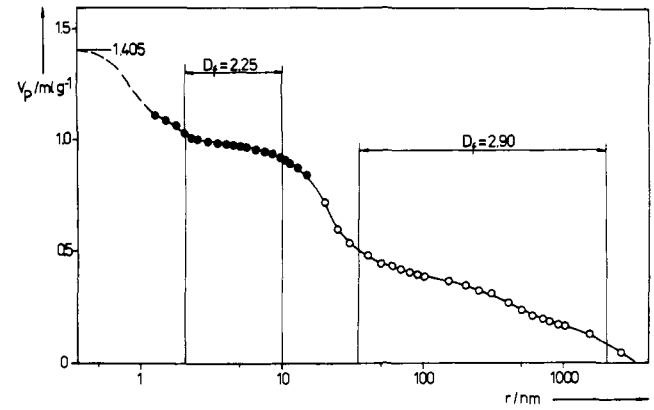

Figure 1. Cummulative pore size distribution $V_p(r)$ of the active carbon Hydraffin 71 as a function of the pore radius r determined from N_2 desorption curves (to 15 nm, ●) and by Hg porosimetry (from 7.5 nm to 7.5 μm, ○). Two different fractal regions are indicated.

For sample preparation, the adsorbent specimens were activated under continuous pumping with a heating rate of 10 K/h up to a final temperature of 400 °C. When the samples were kept for about 10 h under final conditions, the pressure over the sample was less than 10^{-2} Pa. After cooling to room temperature, the adsorbate was introduced into the sample either by chilling from a well-defined volume by means of liquid nitrogen (for propane and *n*-butane as adsorbates) or by means of a microliter syringe (in the case of hexadecane). Afterwards, the adsorbent with the adsorbate was transferred into the NMR sample tubes up to a filling height of about 15 mm. Finally, the tubes were closed hermetically. The diameter of the sample tubes was 8 mm. Within the NMR spectrometer, the temperature of the samples could be varied by a temperature-controlled stream of evaporated nitrogen (for temperatures below room temperature) or by heated air. In this way, a temperature region between −100 and +100 °C could be covered. The accuracy of the temperature adjustment was about 2 K. Depending on the signal-to-noise ratio, the mean error in the observed molecular mean square displacements within the samples is between 20 and 50%.

Results and Discussion

Active Carbon. With application of the conception of fractal dimensions, the seemingly irregular pore size distribution of noncrystalline microporous adsorbents could be shown to follow quite simple relations.[5,21,22] In many cases, the pore size distribution was found to be characterized by one fractal dimension D_f over the whole pore size range, i.e., with the lower cutoffs coinciding with the smallest pore radii and with the upper cutoffs coinciding with the largest pore radii, respectively.[21-23] In particular, in the region between the upper and lower cutoffs, the fractal dimension of the pore model may be determined via the relation[22]

$$D_f \approx 2 - \frac{\Delta \log (\Delta V/\Delta r)}{\Delta \log r} \quad (4)$$

(10) Alexander, S.; Orbach, R. *J. Phys., Lett.* **1982**, *43*, L625.
(11) Kärger, J.; Pfeifer, H. *Zeolites* **1987**, *7*, 90.
(12) Heink, W.; Kärger, J.; Pfeifer, H.; Stallmach, F. *J. Am. Chem. Soc.* **1990**, *112*, 2175.
(13) Kärger, J.; Pfeifer, H.; Vojta, G. *Phys. Rev. A* **1988**, *37*, 4514.
(14) Förste, C.; Heink, W.; Kärger,J.; Pfeifer, H.; Feoktistova, N. N.; Zhdanov, S. P. *Zeolites* **1989**, *9*, 299.
(15) Pfeifer, H. *Phys. Rep.* **1976**, *26*, 293.
(16) Tanner, J. E.; Stejskal, E. O. *J. Chem. Phys.* **1968**, *49*, 1768.
(17) Szargan, P.; Möbius, R.; Spindler, H.; Kraft, M. *Chem. Tech.* (*Leipzig*) **1988**, *40*, 257.
(18) Spindler, H.; Becker, K. *Chem. Tech.* (*Leipzig*) **1990**, *42*, 369.
(19) Zhdanov, S. P.; Khvoshchov, S. S.; Samulevich, N. N. *Synthetic Zeolites*; Khimiya: Moscow, 1981.
(20) Kärger, J.; Pfeifer, H.; Caro, J.; Bülow, M.; Richter-Mendau, J.; Fahlke, B.; Rees, L. V. C. *App. Catal.* **1986**, *24*, 187.
(21) Spindler, H.; Ackerman, W.-G.; Kraft, M. *Z. Phys. Chem.* (*Leipzig*) **1988**, *268*, 1233.
(22) Spindler, H.; Kraft, M. *Catal. Today* **1988**, *3*, 395.
(23) Spindler, H.; Szargan, P.; Kraft, M. *Z. Chem.* **1987**, *27*, 230.

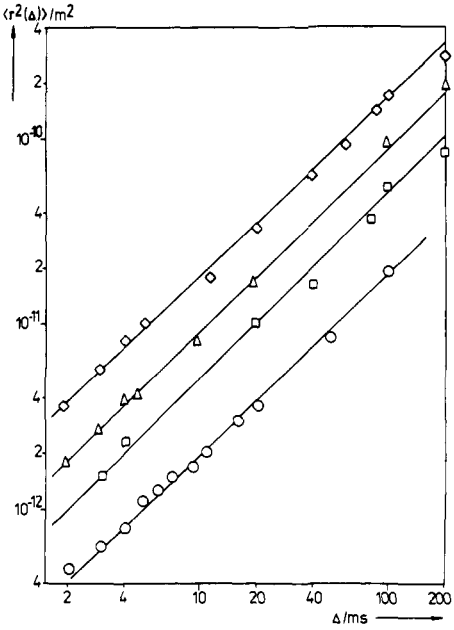

Figure 2. Mean square displacements $\langle r^2(\Delta)\rangle$ of *n*-hexadecane adsorbed on active carbon at a pore filling factor of 0.43 at 291 K (○), 323 K (□), 363 K (△), and 413 K (◇), respectively, in dependence on the observation time Δ. The straight lines indicate the dependence $\langle r^2(\Delta)\rangle \propto \Delta$.

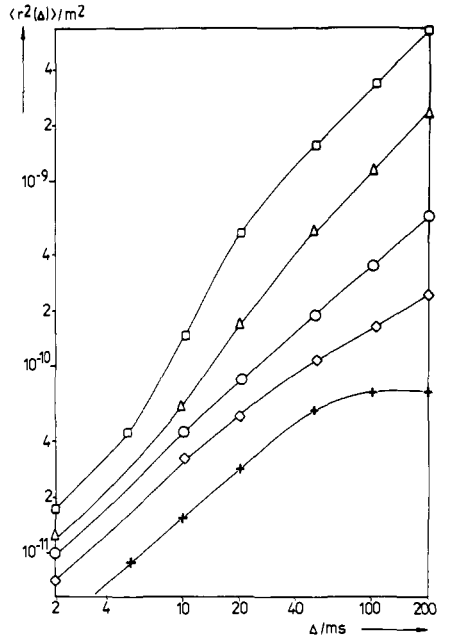

Figure 3. Mean square displacements $\langle r^2(\Delta)\rangle$ of *n*-butane on zeolite NaX with a mean crystallite diameter of 16 μm at a sorbate concentration of 80 mg/g at 183 K (+), 223 K (◇), 243 K (○), 258 K (△), and 273 K (□), respectively, in dependence on the observation time Δ.

It should be noted that, in some cases, the adsorbent must be considered to be composed of different fractal regions. In this case, the pore size distribution is represented by a set of fractal dimensions, each of them characterizing a certain interval of the distribution.

Analysis of Figure 1 on the basis of eq 4 shows that the pore size distribution may be reflected by a fractal pore model over two intervals, namely with the dimension $D_{f(1)} = 2.25$ from 2 to 10 nm, and with $D_{f(2)} = 2.90$ from 30 nm to 2 μm. Figure 2 shows the mean square displacements obtained by PFG NMR for *n*-hexadecane adsorbed on the considered specimen of active carbon for a sorbate concentration of 0.6 mL of hexadecane/g of adsorbent, corresponding to a pore filling factor of 0.43. One may assume, therefore, that the observed mean square displacements are in fact those of the molecules in the interior of the adsorbent pore system, i.e., mean square displacements of molecules migrating under the perpetual influence of the internal structure. In addition, with *n*-hexadecane, we have applied a molecular species whose gas pressure at the temperature of the experiments is so low that any contribution of gas-phase diffusion may be neglected. One has to conclude, therefore, that the observed molecules will in fact remain in perpetual contact with the internal surface of the adsorbent.

Figure 2 shows that, for all temperatures considered, the self-diffusion measurements do not indicate any deviation from ordinary diffusion over the whole range of displacements. In view of the fractal properties of the pore size distribution, one might have expected the occurrence of features of anomalous mass transfer at least in the region of overlap of the measured root mean square displacements with the pore radii. It turns out, however, that evidently even for the minimum displacements observed in the experiments, the majority of the diffusants has not remained within the individual regions of uniform fractal structure. However, as soon as molecular migration will proceed over distances covering several fractal regions, mass transfer may again be understood as a simple Markoffian process leading to proportionality between the mean square displacements and the observation times.[24] This seems to be the case in the present measurements. It is difficult to say what the minimum displacements should be in order to guarantee an observation of anomalous diffusion, and whether in real systems a fractal pore size distribution of an adsorbent should at all necessarily lead to an anomalous diffusion of the molecules adsorbed thereon.

Zeolites. Due to the well-ordered intracrystalline pore structure,[25,26] mass transfer in the interior of the individual zeolite crystallites must be expected to follow Einstein's relation (eq 1) for ordinary diffusion. This prognosis has been confirmed in previous NMR self-diffusion studies[12] and is as well reflected in the diffusion data for *n*-butane in zeolite NaX presented in Figure 3, as long as the root mean square displacements are sufficiently small. In this case, the root mean square displacements are exclusively determined by the intracrystalline diffusivity D_{intra}. However, as soon as the mean diffusion paths covered during the observation time are of the order of the crystallite radii, the influence of the sample heterogeneity becomes significant. Now the relation between $\langle r^2(\Delta)\rangle$ and Δ should also depend on the rate of mass transfer through the crystallite bed, i.e., on the coefficient of long-range self-diffusion D_{lr}.[11] In particular, if additional mass transfer resistances on the zeolite surface ("surface barriers"[11,27]) can be excluded, long-range diffusivities exceeding D_{intra} should lead to deviations to higher mean square displacements, while in the reverse case deviations to lower values should occur. In general, a good estimate of the long-range diffusivity is provided by the relation[11]

$$D_{lr} = p_{inter} D_{inter} \tag{5}$$

with p_{inter} and D_{inter} denoting the relative amount of molecules in the intercrystalline space and their diffusivity, respectively. Thus, the temperature dependence of D_{lr} is mainly given by that of p_{inter}, leading to an activation energy of D_{lr} being of the order of the desorption heat. In most cases, the activation energy of intracrystalline diffusion is smaller than the heat of desorption so that D_{lr} increases faster than D_{intra} with increasing temperature. This behavior is reflected in the experimental data given in Figure 3, which for temperatures $T < 223$ K show a deflection of $\langle r^2(\Delta)\rangle$ to lower values (i.e., the behavior expected for $D_{lr} < D_{intra}$), and the reverse behavior for larger temperatures ($T > 258$K). Obviously, for $T \approx 243$ K, the coefficients of intracrystalline and long-range diffusion are of the same order of magnitude. Applying

(24) Spindler, H.; Kärger, Z. *Phys. Chem.* (*Leipzig*) **1989**, *270*, 225.

(25) Breck, D. W. *Zeolite Molecular Sieves*; Wiley: New York, 1974.
(26) Ruthven, D. M. *Principles of Adsorption and of Adsorption Processes*; Wiley: New York, 1984.
(27) Bülow, M. *Kolloidn. Zh.* **1978**, *40*, 207.

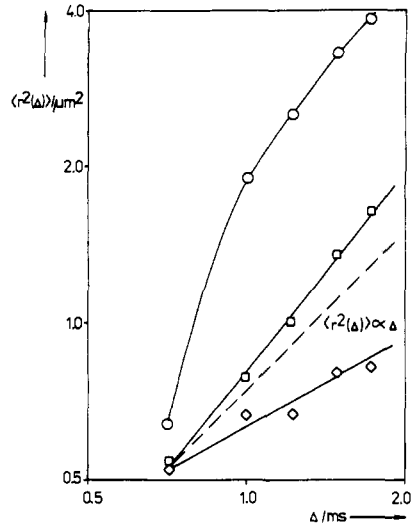

Figure 4. Mean square displacements $\langle r^2(\Delta)\rangle$ of propane on polycrystalline grains of zeolite ZSM-5 after different coking times for a sorbate concentration of 2.5 molecules per $^1/_4$ unit cell at 296 K in dependence on the observation time for the fresh zeolite (○) and after coke deposition (□, 3.6 mass %, obtained after 1 h coking; ◇, 4.3 mass %, obtained after 12 h coking, recalculated from the diffusion data of ref 28. The broken line indicates the dependence $\langle r^2(\Delta)\rangle \propto \Delta$.

eq 1 yields a value of 8.3×10^{-10} m^2 s^{-1}.

It is evident that a measurement of the mean square displacement over a limited range of observation times—and in particular over such observation times for which $\langle r^2(\Delta)\rangle$ is of the order of the mean square crystallite radii, i.e., in our case of 64 $\times 10^{-12}$ m^2—leads to dependences as given by eq 2, where for $T > 243$ K one has $\varkappa > 1$, and for $T < 243$ K $\varkappa < 1$, respectively. These deviations from ordinary diffusion are obviously brought about by the heterogeneity of the system, i.e., by the change in the migration modes as soon as the molecules pass from the interior of the crystallites to the intercrystalline space.

If the individual particles are polycrystalline grains rather than monocrystals, such a behavior may be expected to occur also for migration paths within the adsorbent particles, as soon as the space between the individual crystallites of the grains allows a promotion of molecular migration. The formation of polycrystalline particles is typical of zeolite ZSM-5. Determining the mean square displacements from the self-diffusion data of propane in such samples[28] does in fact lead to the expected deviation from ordinary diffusion, as shown in Figure 4. As a consequence of the short transverse nuclear magnetic relaxation times (in the present case, about 0.5 ms), the measuring conditions for ZSM-5 are much poorer than for the other adsorbents considered. The observation time could therefore only be varied from 0.7 to 1.7 ms. It should be mentioned, however, that diffusion measurements with propane on ZSM-5 monocrystals over the same range of observation times did in fact yield clear evidence of ordinary diffusion.[20] Figure 4 shows the molecular mean square displacements in the starting sample as well as in samples with coke depositions in the interior of the polycrystalline grains (cf. ref 28). It turns out that, in the starting material, molecular migration seems to be promoted by the existence of some free space between the individual crystallites. This means that, with increasing observation time, more and more molecules should be able to participate in the faster motion outside the crystallites. This situation is obviously reversed by the coke depositions whose influence leads to a continuous retardation of mass transfer with increasing observation time.

Conclusion

In active carbon microporous adsorbents, whose nonuniform pore structure may be satisfactorily described by fractal pore models, molecular mass transfer as observed by PFG NMR does not yield any indication of anomalous diffusion as to be expected for mass transfer upon lattices of fractal geometry. By contrast, PFG NMR self-diffusion measurements of molecules adsorbed on zeolites may be shown to trace deviations from a linear relationship between the mean square displacement and the observation time. However, this may be referred to the influence of mass transfer through the intercrystalline space, which may become significant as soon as the molecular mean square displacements are of the order of or larger than the crystalline dimensions. It is most likely that the deviation from ordinary diffusion as observed for mass transfer within polycrystalline grains may be explained by an equivalent mechanism.

Acknowledgment. We thank Profs. Harry Pfeifer, Peter Pfeifer, and Günter Vojta as well as Dr. Jürgen Caro for stimulating discussions.

Registry No. C, 7440-44-0; PrH, 74-98-6; BuH, 106-97-8; hexadecane, 544-76-3.

(28) Völter, J.; Caro, J.; Bülow, M.; Fahlke, B.; Kärger, J.; Hunger, M. *Appl. Catal.* **1988**, *42*, 15.